Intracellular observation of nanocarriers modified with a mitochondrial targeting signal peptide

*Eriko Kawamura[1,3], Yuma Yamada[1,3], Yukari Yasuzaki[1], Mamoru Hyodo[2], Hideyoshi Harashima[1,2,]**

[1] Laboratory for Molecular Design of Pharmaceutics, Faculty of Pharmaceutical Sciences, Hokkaido University, Kita-12, Nishi-6, Kita-ku, Sapporo 060-0812, Japan

[2] Laboratory of Innovative Nanomedicine, Faculty of Pharmaceutical Sciences, Hokkaido University, Kita-12, Nishi-6, Kita-ku, Sapporo 060-0812, Japan

[3] These authors contributed equally as first author

*To whom correspondence should be addressed: Laboratory for Molecular Design of Pharmaceutics, Faculty of Pharmaceutical Sciences, Hokkaido University, Kita-12, Nishi-6, Kita-ku, Sapporo 060-0812, Japan. E-mail: harasima@pharm.hokudai.ac.jp. Phone: +81-11-706-3919. Fax: +81-11-706-4879

Keywords: *Mitochondria; Mitochondrial drug delivery; Mitochondrial targeting signal peptide (MTS); MITO-Porter; Nanocarriers; Nanotechnology.*

Abstract

This study focused on the intracellular observation of nanocarriers modified with a mitochondrial targeting signal peptide (MTS). The nanocarriers showed an efficient cellular uptake, and the MTS had a positive effect on their mitochondrial targeting. This is the first report of an intracellular observation of nanocarriers modified with MTS.

Main text

Innovative medicine development would be accelerated by the nanocarriers that target a specific organelle, such as the nucleus, mitochondria, the golgi apparatus, the endoplasmic reticulum, all of which are promising targets for therapeutic drugs. Mitochondria are intimately involved in maintaining the homeostasis of vital physiological functions (1) and a dysfunction is a causative factor in a variety of human diseases (2-4). Thus, mitochondria represent a promising therapeutic target, and the delivery of a wide variety of molecules have been reported to date (5-7). The use of an organelle targeting signal tag would make it possible to selectively deliver exogenous proteins and RNA to mitochondria (8-11). However, the issue of whether these signal tags would be useful ligands for the targeting of a nanoparticle with a diameter of more than 100 nm to a specific target has not been demonstrated to date.

In a previous study, we reported on the development of nanocarriers equipped with a mitochondrial targeting signal peptide (MTS), which permits the selective delivery of certain types of proteins to mitochondria. The nanocarriers were then used to determine if MTS would be a useful ligand for the selective mitochondrial delivery of a nanoparticle (12). In that study, using cell homogenates, we observed that MTS-modified liposomes efficiently accumulated in mitochondria. While the results indicated that MTS has the potential for functioning as a ligand for nanoparticles, the utility of such signal tags have not yet been demonstrated in living cells.

The purpose of this study was to validate whether the presence of MTS on a surface of a nanoparticle enhances their targeting to mitochondria, as well as endogenous mitochondrial proteins

in living cells. We report herein on the intracellular observation of an MTS-modified nanocarrier using the Dual Function (DF)-MITO-Porter system, which permits the efficient cytosolic delivery of MTS-modified nanocarriers to be achieved (13-15). We first attempted to develop a DF-MTS-MITO-Porter modified with MTS, and optimized the preparation. The cellular uptake efficiency of the carriers was evaluated by means of flow cytometry analyses. Intracellular observations using confocal laser scanning microscopy (CLSM) permitted us to compare the DF-MTS-MITO-Porter and DF-R8-MITO-Porter, a conventional DF-MITO-Porter, in terms of mitochondrial targeting.

To observe the intracellular trafficking of MTS-modified nanocarriers, we attempted to construct a DF-MTS-MITO-Porter, by a high density of octaarginine (R8)-modification to enhance cellular uptake (16), incorporating an endosome-fusogenic lipid envelope for endosomal escape (17, 18) and the MITO-Porter for mitochondrial delivery (14, 19). The construction of the DF-MTS-MITO-Porter involved the following three steps: (1) the preparation of a mitochondria-fusogenic envelope equipped with maleimide polyethylene glycol (Mal-PEG); (2) modification of the envelope with an MTS-Cys peptide (NH_2-MVSGSSGLAAARLLSRTFLLQQNGIRHGSYC) (Hokkaido System Science Co., Ltd; Sapporo, Japan) to produce a MTS-MITO-Porter; (3) further step-wise coating with an endosome-fusogenic envelope (Fig. 1A).

We first prepared the MTS-MITO-Porter by the lipid film hydration method, as previously reported (19), and the particle-diameters and ζ potentials were determined using Zetasizer Nano ZS (Malvern Instruments, Herrenberg, Germany). The envelopes were composed of 1, 2-dioleoyl-sn-glycero-3-phosphatidyl ethanolamine (DOPE)/sphingomyelin (SM)/DOPE-N-[4-(p-maleimidomethyl)cyclohexane-carboxamide] (Mal-DOPE) [9:2:0.5], and were modified with MTS-Cys at levels of 0.5, 1.0, 2.5, 5 mol% of the total lipid. DOPE and Mal-DOPE were purchased from Avanti Polar lipids (Alabaster, AL, USA). SM was purchased from Sigma (St. Louis, MO, USA). The modification of the MTS peptide resulted in a gradual increase in the diameter of the MITO-Porter, and aggregation occurred when with MTS exceeded 2.5 mol% (Table S1). This tendency

corresponded to a previous report showing that it is difficult to maintain envelope-structures in the presence of high densities of the MTS peptide (12). To overcome this problem, we used 1,2-distearoyl-sn-glycero-3-phosphoethanolamine-N-Mal-PEG (Mal-PEG-DSPE) (Nippon Oil and Fats Co.; Tokyo, Japan) as an anchor between the MTS-peptide and the envelopes of the MITO-Porter. It was expected that modifying the surface of the lipid envelope with PEG would increase dispersibility to inhibit the aggregation that occurred during the preparation of the MTS-MITO-Porter. This procedure permitted the construction of a MTS-MITO-Porter, with a diameter of less than 100 nm (Table S1).

While it is well known that MTS has a high mitochondrial targeting activity, no reports regarding cellular uptake have appeared. In this study, we first investigated the cellular uptake efficiency of the R8-MITO-Porter and the MTS-MITO-Porter. The cellular uptakes of the carriers with inner lipid envelopes labeled with 1% 7-nitrobenz-2-oxa-1, 3-diazole (NBD) labeled DOPE (Avanti Polar lipids) were evaluated using flow cytometry, as previously reported (20). Briefly, the carriers were added to HeLa human cervix carcinoma cells (RIKEN Cell Bank, Tsukuba, Japan) (final inner lipid concentration, 9.2 μM), and the cells were then incubated in serum-free Dulbecco's modified Eagle medium (DMEM) (Invitrogen Corporation; Carlsbad, CA, USA) for 1 hr under an atmosphere of 5% CO_2/air at 37ºC. After the incubation, the cells were then analyzed by using flow cytometry (FACScan, Becton Dickinson, Franklin Lakes, NJ, USA) and the CellQuest software (Becton Dickinson). The cellular uptake of the carriers were expressed as the mean fluorescence intensity, calculated using the Cell Quest software (Becton Dickinson). The percentages of cells with carriers were also calculated (see Figure S1 for the details). The results show that the cellular uptake of the MTS-MITO-Porter was significantly lower than that of the R8-MITO-Porter (Fig. 1B), and the percentages of cells with the MTS-MITO-Porter and the R8-MITO-Porter were 0.3% and 99.7%, respectively (Fig. S1A), indicating that mitochondrial targeting using the MTS-MITO-Porter in living cells requires cellular uptake.

To achieve cytosolic delivery of the MTS-MITO-Porter, we attempted to use the DF-MITO-Porter system. For packaging the MTS-MITO-Porter, the outer envelope had an endosome-fusogenic composition [DOPE/phosphatidic acid (PA)/Stearyl-R8 (7:2:2, molar ratio)] (17, 18) by the multi-layering method (Fig. 1A), as previously reported (13, 17). Stearyl R8 was obtained from Kurabo Industries Ltd (Osaka, Japan) in the purified form. PA was purchased from Sigma. The MTS-MITO-Porter was packaged with outer envelopes through the membrane fusion of neighboring R8-modified small unilamellar vesicles (SUVs), triggered by the assembly of the positive charged R8-SUVs (about +30 mV in Table S2) around the negatively charged MTS-MITO-Porter (about -20 mV in Table 1) to reverse the surface charge (about +20 mV in Table 1). The conversion of the ζ potential in the coating process strongly suggests that the MTS-MITO-Porter was packaged with outer envelopes modified with R8. While, R8-MITO-Porter was packaged with outer envelopes, triggered by the assembly of negative charged SUVs (about -50 mV in Table S2) around the positive charged R8-MITO-Porter (about +50 mV in Table 1), and a stearyl R8 solution (10 mol% of SUV lipid) was then added to the resulting suspension to modify the outer envelope with R8, as shown in our previously report (15, 17, 20). As shown in Figure 1C, the efficiencies of cellular uptake for the DF-MTS-MITO-Porter and DF-R8-MITO-Porter were similar, even though the inner ligands were different. The percentages of cells with the DF-MTS-MITO-Porter (99.8%) and the DF-R8-MITO-Porter (99.6%) were similar (Fig. S1B). Based on these results, we concluded that the DF-MITO-Porter system permitted the efficient cellular uptake the MTS-MITO-Porter.

To evaluate the mitochondrial targeting activity of the MTS-MITO-Porter in living cells, we observed the intracellular trafficking of the DF-MTS-MITO-Porter in which the inner lipid envelope was labeled with 1% NBD-DOPE (green) after staining mitochondria red by CLSM, as previously reported (20). Briefly, the carriers were added to HeLa cells (final inner lipid concentration, 9.2 μM), and the cells were then incubated in phenol red-free DMEM (Invitrogen) without serum under an atmosphere of 5% CO_2/air at 37ºC. After a 1-hr incubation, the medium was replaced with fresh

phenol red-free DMEM containing 10 % fetal bovine serum (FBS) (Thermo Scientific, Waltham, MA, USA), and the cells were incubated in the absence of the carriers for 2 hr. The cells were observed by CLSM (LSM510, Carl Zeiss Co. Ltd., Jena, Germany) after staining the mitochondria in the medium containing MitoFluorRed589 (Invitrogen Corporation). We also calculated the mitochondrial targeting activity of the carriers, as previously reported (20) (see Table S3 for the details).

As a result, no signals corresponding to the MTS-MITO-Porter without an outer R8-modified envelope was observed (Fig. 2B), while the R8-MITO-Porter were observed inside cells and weakly localized in red stained mitochondria (Fig. 2A). This result is in agreement with the cellular uptake analysis shown in Figures 1A, 1B. In the case of the DF-MITO-Porter system, both the DF-MTS-MITO-Porter and the DF-R8-MITO-Porter were co-localized with mitochondria, observed as a yellow signal (Fig. 2C, D), and the mitochondrial targeting activities of the DF-MTS-MITO-Porter and DF-R8-MITO-Porter were 24% and 16%, respectively (Table S3). The results indicate that the MTS peptide functions as a mitochondrial targeting ligand of nanocarriers in living cells, and that the mitochondrial targeting of the MTS-peptide is enhanced slightly compared with that of the R8-MITO-Porter.

However, mitochondrial targeting by MTS failed to result in the selective mitochondrial delivery of nanocarriers that were quite different from that of proteins, which are its original cargoes. We previously showed that MTS enhanced the mitochondrial targeting of nanoparticles in cell homogenates (12), however this was not the case, when living cells were used. We conclude that this contradiction was largely the result of the cell environment, where there are many cytoskeletons and a high density of cell components inside the cells. MTS selectively imports the original protein to mitochondria in living cells. While, it would be difficult for MTS to selectively deliver a nanocarrier to mitochondria, because, in the case of large-sized cargoes, mitochondrial import by MTS might be inhibited by many intracellular barriers. Thus, the mitochondrial delivery of a nanocarrier by MTS

needs to be improved, in terms of the intracellular dispersibility of the nanocarrier in living cells. Cytoskeletons such as actin filaments and microtubules, represent a potential tool for delivering a nanocarrier.

The findings reported herein show that PEG permitted MTS to be combined with a mitochondrial fusogenic nanocarrier. When used in combination with the DF-MITO-Porter system, the MTS-MITO-Porter was taken up extensively by cells. Our findings also provide information regarding the intracellular trafficking of a nanocarrier equipped with an organelle targeting signal tag, and we found issues for organelle selective targeting of nanocarrier in living cells. If it were possible to prepare a nanocraft that could specifically target a specific organelle, this would open a new field of research directed toward therapy for various diseases. Studies directed toward this goal are currently underway.

Acknowledgments

This work was supported, in part by, the Program for Promotion of Fundamental Studies in Health Sciences of the National Institute of Biomedical Innovation, Japan (NIBIO), a Grant-in-Aid for Young Scientists (A) and a Grant-in-Aid for Scientific Research (S) from the Ministry of Education, Culture, Sports, Science and Technology of Japanese Government (MEXT). We also thank Milton Feather for his helpful advice in writing the manuscript.

References

1. **Szewczyk, A. and Wojtczak, L.:** Mitochondria as a pharmacological target, Pharmacol. Rev., **54**, 101-127: (2002).
2. **Chan, D.C.:** Mitochondria: dynamic organelles in disease, aging, and development, Cell, **125**, 1241-1252: (2006).
3. **Reeve, A.K., Krishnan, K.J. and Turnbull, D.:** Mitochondrial DNA mutations in disease, aging, and neurodegeneration, Ann. N. Y. Acad. Sci., **1147**, 21-29: (2008).
4. **Schapira, A.H.:** Mitochondrial disease, Lancet, **368**, 70-82: (2006).

5. **Zhang, E., Zhang, C., Su, Y., Cheng, T. and Shi, C.:** Newly developed strategies for multifunctional mitochondria-targeted agents in cancer therapy, Drug Discov. Today, **16**, 140-146: (2011).

6. **Yamada, Y. and Harashima, H.:** Mitochondrial drug delivery systems for macromolecule and their therapeutic application to mitochondrial diseases, Adv. Drug Deliv. Rev., **60**, 1439-1462: (2008).

7. **Mukhopadhyay, A. and Weiner, H.:** Delivery of drugs and macromolecules to mitochondria, Adv. Drug Deliv. Rev., **59**, 729-738: (2007).

8. **Schatz, G.:** The protein import system of mitochondria, J. Biol. Chem., **271**, 31763-31766: (1996).

9. **Vestweber, D. and Schatz, G.:** DNA-protein conjugates can enter mitochondria via the protein import pathway, Nature, **338**, 170-172: (1989).

10. **Rubio, M.A., Rinehart, J.J., Krett, B., Duvezin-Caubet, S., Reichert, A.S., Soll, D. and Alfonzo, J.D.:** Mammalian mitochondria have the innate ability to import tRNAs by a mechanism distinct from protein import, Proc. Natl. Acad. Sci. U. S. A., **105**, 9186-9191: (2008).

11. **Wang, G., Chen, H.W., Oktay, Y., Zhang, J., Allen, E.L., Smith, G.M., Fan, K.C., Hong, J.S., French, S.W., McCaffery, J.M., and other 3 authors:** PNPASE regulates RNA import into mitochondria, Cell, **142**, 456-467: (2010).

12. **Yamada, Y. and Harashima, H.:** Enhancement in selective mitochondrial association by direct modification of a mitochondrial targeting signal peptide on a liposomal based nanocarrier, Mitochondrion: (2012). (in press)

13. **Yamada, Y., Furukawa, R., Yasuzaki, Y. and Harashima, H.:** Dual function MITO-Porter, a nano carrier integrating both efficient cytoplasmic delivery and mitochondrial macromolecule delivery, Mol. Ther., **19**, 1449-1456: (2011).

14. **Yamada, Y., Akita, H. and Harashima, H.:** Multifunctional envelope-type nano device (MEND) for organelle targeting via a stepwise membrane fusion process, Methods Enzymol., **509**, 301-326: (2012).

15. **Yamada, Y. and Harashima, H.:** Delivery of bioactive molecules to the mitochondrial genome using a membrane-fusing, liposome-based carrier, DF-MITO-Porter, Biomaterials, **33**, 1589-1595: (2012).

16. **Khalil, I.A., Kogure, K., Futaki, S. and Harashima, H.:** High density of octaarginine stimulates macropinocytosis leading to efficient intracellular trafficking for gene expression, J. Biol. Chem., **281**, 3544-3551: (2006).

17. **Akita, H., Kudo, A., Minoura, A., Yamaguti, M., Khalil, I.A., Moriguchi, R., Masuda, T., Danev, R., Nagayama, K., Kogure, K. and Harashima, H.:** Multi-layered nanoparticles for penetrating the endosome and nuclear membrane via a step-wise membrane fusion process, Biomaterials, **30**, 2940-2949: (2009).

18. **El-Sayed, A., Khalil, I.A., Kogure, K., Futaki, S. and Harashima, H.:** Octaarginine- and octalysine-modified nanoparticles have different modes of endosomal escape, J. Biol. Chem., **283**, 23450-23461: (2008).

19. **Yamada, Y., Akita, H., Kamiya, H., Kogure, K., Yamamoto, T., Shinohara, Y., Yamashita, K., Kobayashi, H., Kikuchi, H. and Harashima, H.:** MITO-Porter: A liposome-based carrier system for delivery of macromolecules into mitochondria via membrane fusion, Biochim. Biophys. Acta, **1778**, 423-432: (2008).

20. **Yamada, Y., Kawamura, E. and Harashima, H.:** Mitochondrial-targeted DNA delivery using a DF-MITO-Porter, an innovative nano carrier with cytoplasmic and mitochondrial fusogenic envelopes, J. Nanopart. Res., **14**, 1-15: (2012).

Figure legends

Fig. 1 Schematic diagram of the preparation of the MTS-MITO-Porter and DF-MTS-MITO-Porter (A). MTS, mitochondrial targeting signal peptide; PEG, polyethylene glycol; STR-R8, stearyl octaarginine; R8-SUV, R8-modified small unilamellar vesicles. The cellular uptake of the MITO-Porter (B) and the DF-MITO-Porter (C) with inner lipid envelopes labeled with 1% NBD-lipids were evaluated using flow cytometry. Data are represented as the mean ± S.D. (n = 3). *Significant difference ($p < 0.01$ by one-way ANOVA, followed by Student-Newman-Keuls (SNK) test).

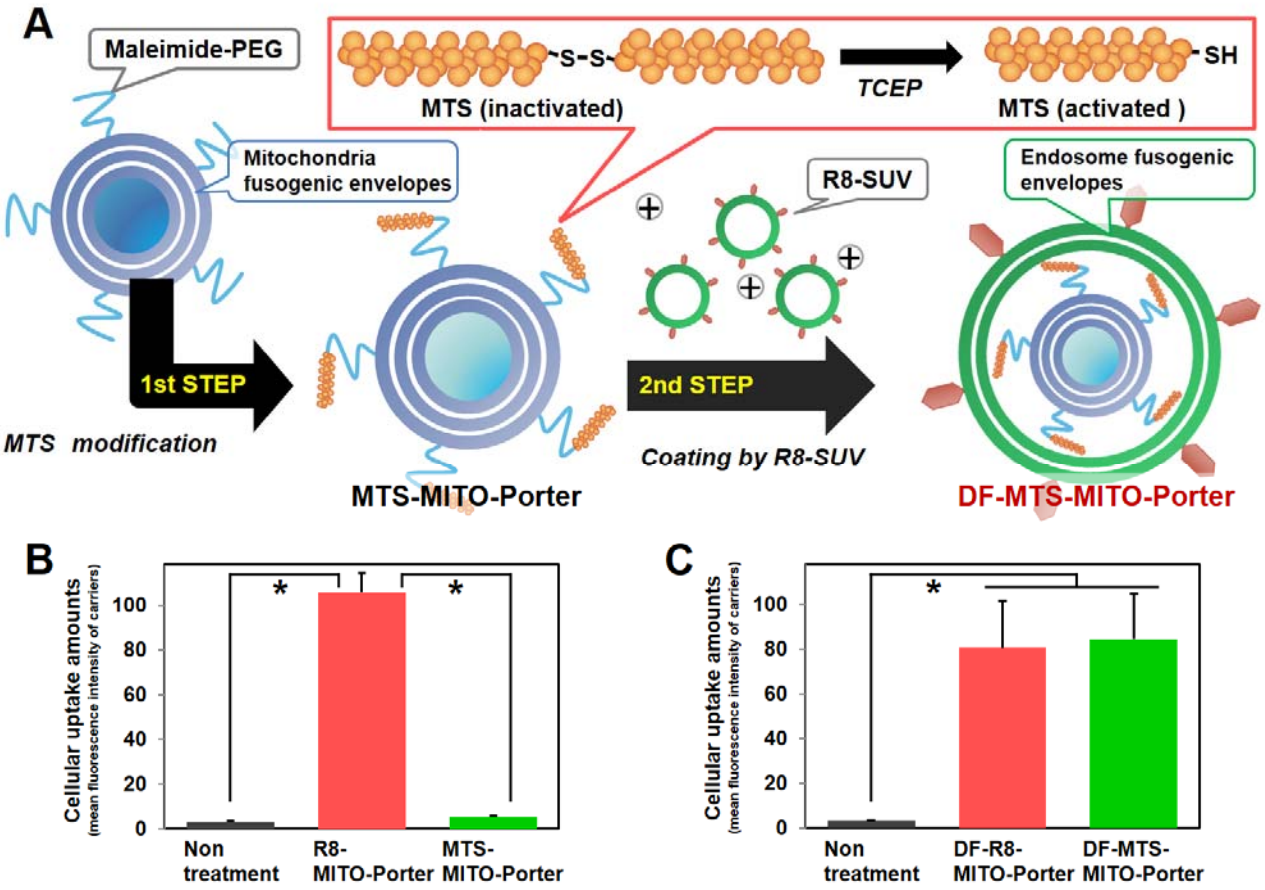

Fig. 2 Intracellular observation of carriers. The intracellular trafficking of the carriers with inner lipid envelopes labeled with 1% NBD-lipids (green) was observed using CLSM, after staining the mitochondria with Mitofluor Red 589 (red). The carrier (green) was observed to co-localize with red stained mitochondria, observed as a yellow signal. A, MTS-MITO-Porter; B, R8-MITO-Porter; C, DF-MTS-MITO-Porter; D, DF-R8-MITO-Porter. Scale bars, 10 μm.

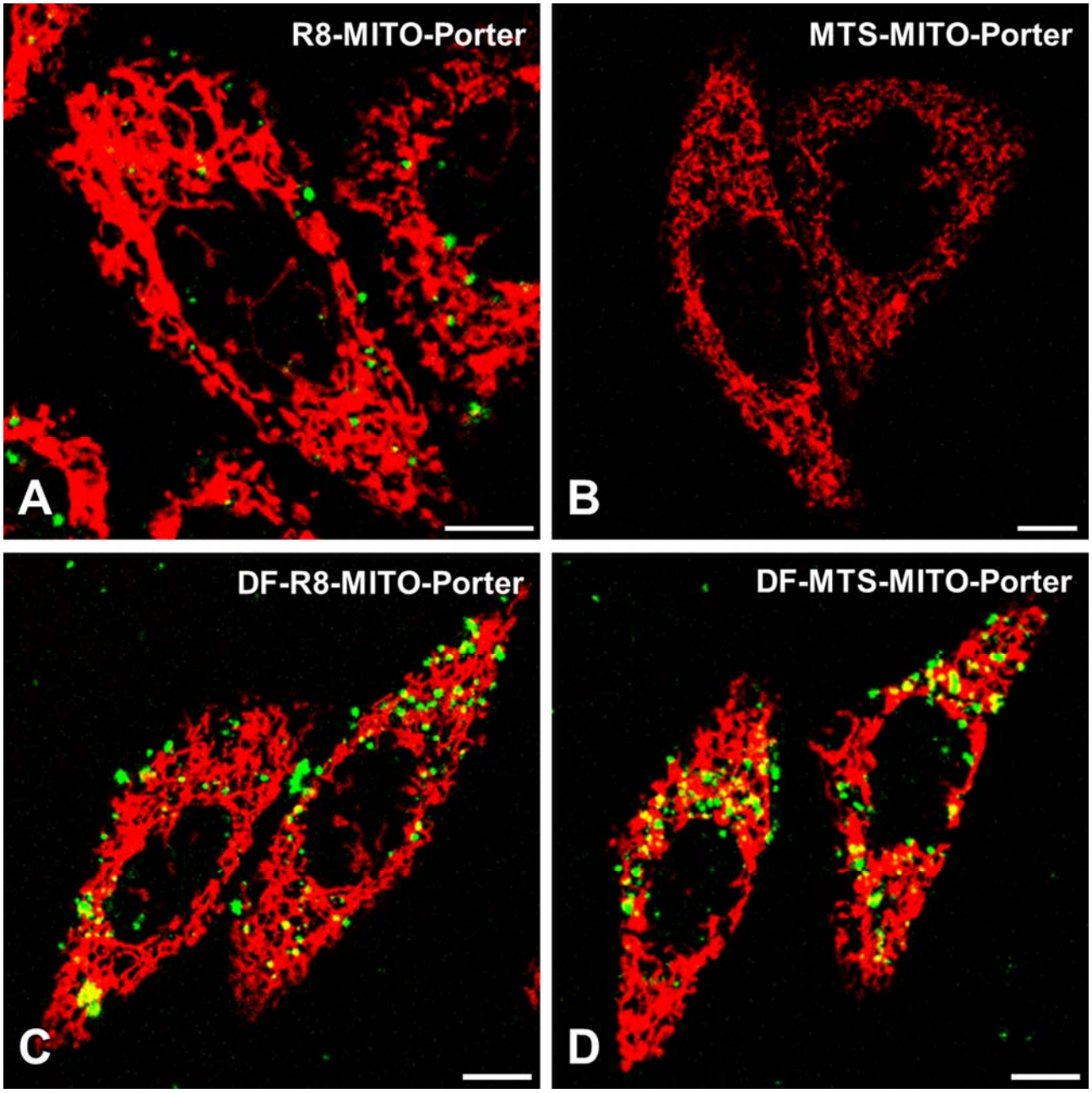

Table 1

Physicochemical properties of the MITO-Porter and the DF-MITO-Porter

	Lipid composition of inner envelopes [molar ratio]	Diameter (nm)		PDI		ζ potential (mV)	
		Conventional	DF	Conventional	DF	Conventional	DF
DF-MTS-MITO-Porter	DOPE/SM/Mal-PEG-DSPE/MTS-Cys [9:2:0.5:0.25]	91 ± 6	102 ± 16	0.324 ± 0.070	0.233 ± 0.006	-21 ± 9	22 ± 18
	DOPE/SM/Mal-PEG-DSPE/MTS-Cys [9:2:0.5:0.5]	87 ± 5	92 ± 9	0.283 ± 0.024	0.206 ± 0.015	-19 ± 11	20 ± 5
DF-R8-MITO-Porter	DOPE/SM/Stearyl R8 [9:2:1]	117 ±15	142 ± 12	0.267 ± 0.048	0.180 ± 0.019	54 ± 6	50 ± 9

mean ± S.D. n=3-10

Supplementary data

Fig. S1 Evaluation of the cellular uptake of carriers. Representative flow cytometry histograms of the cellular uptake of the MITO-Porter (A) and the DF-MITO-Porter (B). Histograms in green and red indicate MTS-modified carriers and R8-modified carriers, respectively. M1, cells with no carrier uptake [region corresponding to 99.9% of no treated cells (histogram in black)]. M2, cells with carriers. The percentages of cells in the region M2 represent the average of three independent experiments.

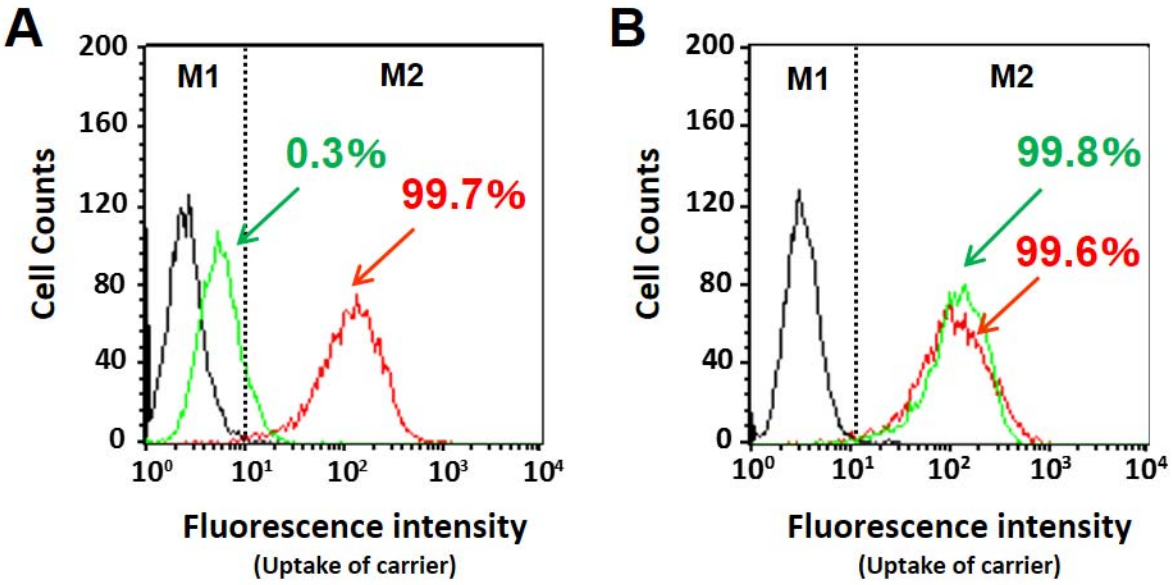

Table S1. Characteristics of MTS-MITO-Porter

Lipid composition of envelopes	MTS modification rate (%)	Diameter (nm)	PDI	ζ pote
DOPE/SM/Maleimide-DOPE [9:2:0.5]	0	111 ± 7	0.294 ± 0.060	-
	0.5	99 ± 27	0.243 ± 0.037	-
	1	204 ± 190	0.396 ± 0.258	-
	2.5	3444 ± 904	0.824 ± 0.183	-
	5	5282 ± 834	0.758 ± 0.229	-
DOPE/SM/Maleimide-PEG-DSPE [9:2:0.5]	0	88 ± 3	0.287 ± 0.041	-
	2.5	91 ± 6	0.324 ± 0.070	-
	5	87 ± 5	0.283 ± 0.024	-1

PDI, polydispersity index. Data are represented by the mean± S.D. (n = 3-10).

Table S2. Characteristics of SUV and R8-SUV

	Lipid compositions	Diameter (nm)	PDI	ζ pote
SUV	DOPE/PA (7/2, molar ratio)	51 ± 3	0.296 ± 0.042	-4
R8-SUV	DOPE/PA/Stearyl R8 (7/2/2, molar ratio)	90 ± 6	0.225 ± 0.027	28

PDI, polydispersity index. Data are represented by the mean± S.D. (n = 4-6).

Table S3. Mitochondrial targeting activity of DF-MTS-MITO-Porter and DF-R8-MITO-Porter

	Mitochondrial targeting activity (%)
DF-MTS-MITO-Porter	24 ± 8
DF-R8-MITO-Porter	16 ± 7

Data are represented by the mean± S.D. (n = 4-5).

The mitochondrial targeting activity was calculated, as previously reported (1). Fluorescent and bright-field images for mitochondria that had been stained were captured, as shown in Figure 2. Each 8-bit TIFF image was analyzed using the Image-Pro plus v.7.0 software (Media Cybernetics, Inc., Bethesda, MD) to quantify the total brightness of each region of interest. First, the yellow pixel areas where carriers (green color) co-localized with mitochondria (red color) were marked in each image. We then counted only clusters with sizes of more than 10 pixels of the signal area. The yellow and green pixel areas of each cluster in the mitochondria, s_i(mt) and the outside of mitochondria, s_i(out), were separately summed for each image, and are denoted as S' Z=j(mt), S' Z=j(out), respectively. The values of S' Z=j(mt) and S' Z=j(out) in each image were further summed and are denoted as S(mt) and S(out), respectively. These parameters represent the total amount of carriers inside and outside the mitochondria in the total cell. Furthermore, the total area of the carrier, denoted as S(tot), was calculated by integrating the S(mt) and S(out). This value represents the total cellular uptake of carrier. The mitochondrial targeting activity was calculated as S(mt) divided by S(tot).

References

1. **Yamada, Y., Kawamura, E. and Harashima, H.:** Mitochondrial-targeted DNA delivery using a DF-MITO-Porter, an innovative nano carrier with cytoplasmic and mitochondrial fusogenic envelopes, J. Nanopart. Res., **14,** 1013: (2012).